Bioorg. Med. Chem. Lett. 45 (2021) 128135

Contents lists available at ScienceDirect

Bioorganic & Medicinal Chemistry Letters

journal homepage: www.elsevier.com/locate/bmcl

Synthesis of propargylamine mycophenolate analogues and their selective cytotoxic activity towards neuroblastoma SH-SY5Y cell line

Patamawadee Silalai [a], Dumnoensun Pruksakorn [b,c], Arthit Chairoungdua [d], Kanoknetr Suksen [d], Rungnapha Saeeng [a,e,*]

[a] Department of Chemistry and Center for Innovation in Chemistry, Faculty of Science, Burapha University, Chonburi 20131, Thailand
[b] Musculoskeletal Science and Translational Research Center, Department of Orthopedics, Faculty of Medicine, Chiang Mai University, Chiang Mai, Thailand
[c] Omics Center for Health Sciences, Faculty of Medicine, Chiang Mai University, Thailand
[d] Department of Physiology, Faculty of Science, Mahidol University, Bangkok 10400, Thailand
[e] The Research Unit in Synthetic Compounds and Synthetic Analogues from Natural Product for Drug Discovery (RSND), Burapha University, Chonburi 20131, Thailand

ARTICLE INFO

Keywords:
A^3-coupling reaction
Cytotoxic activity
Mycophenolic Acid
Molecular docking
Neuroblastoma SH-SY5Y cells
Propargylamine mycophenolate

ABSTRACT

Twenty six propargylamine mycophenolate analogues were designed and synthesized from mycophenolic acid **1** employing a key step A^3-coupling reaction. Their cytotoxic activity was examined against six cancer cell lines. Compounds **6a**, **6j**, **6t**, **6u**, and **6z** exhibited selective cytotoxicity towards neuroblastoma (SH-SY5Y) cancer cells and were less toxic to normal cells in comparison to the lead compound, MPA **1** and a standard drug, ellipticine. Molecular docking results suggested that compound **6a** is fit well in the key amino acid of three proteins (CDK9, EGFR, and VEGFR-2) as targets in cancer therapy. The propargylamine mycophenolate scaffold might be a valuable starting point for development of new neuroblastoma anticancer drugs.

Cancer is an important category of human diseases accounting for an estimated 9.6 million deaths in 2018 (WHO).[1] Synthesis of selective anticancer agents has attracted much research.[2] Recently, therapies have focused on reducing cancer toxicity to specific molecular targets and damage to normal cells.[3] Neuroblastoma, despite some successes remains a challenging region for treatment *via* surgical resection, chemotherapy, or radiation therapy.[4,5] Neuroblastoma is one of the most common solid tumors inflicting children and responsible for approximately 9–15% of pediatric cancer deaths[6] and remains one of the most difficult cancers to cure.[7] Standard treatment for neuroblastoma is based on a combination of drugs such as doxorubicin, vincristine, cyclophosphamide, and cisplatin.[8] Although highly beneficial chemotherapy lacks selectivity towards cancer cells and has severe side effects. To this end there is an urgent need for drugs with greater efficacy and target specificity.[9]

Mycophenolic acid (MPA) is an early antibiotic drug derived from *Penicillium*.[10] It consists of a phthalide in which an aromatic ring is substituted of hydroxy, methyl, methoxy, and six-carbon chain with a double bond in the *trans* configuration and the free carboxylic acid.[11] MPA is a highly noteworthy inhibitor of inosine monophosphate dehydrogenase (IMPDH), a key enzyme in the *de novo* synthesis of guanine nucleotide that causes a suppression of lymphocyte activity in humans and organ rejection in patients who have undergone transplantation.[12,13] MPA was approved for use against organ rejection in USA in 1995.[14] Although most research has focused on their inhibitory immunosuppressive properties,[15–17] recent rekindled interest has focused on the synthesis of novel mycophenolate derivatives in regards their anticancer potency.[18–20] IMPDH receptors are overexpressed in cancer cells compared to normal cells. Inhibition of IMPDH can inhibit proliferation of and induce apoptosis in cancer cells.[21] This suggests MPA and derivatives might function as improved anticancer agents. MPA was found as a potential antiproliferative agent, however MPA therapy is associated with gastrointestinal (GI) adverse events.[22–24] The incidence of MPA-related GI adverse events ranges from 45 to 80% in recipients.[25,26] Therefore, we designed and synthesized of new MPA analogues by esterification of free carboxylic group of MPA **1** to mycophenolate **2** (Scheme 1) and propargylation at phenolic position (Scheme 3) and their use as a structural core for further modification to a series of propargylamine mycophenolate analogues to reduce GI toxicity affects.

The propargylamine moiety (Fig. 1) occurs in therapeutic active agents[27,28] such as rasagiline and deprenyl that show highly selective

* Corresponding author at: Department of Chemistry and Center for Innovation in Chemistry, Faculty of Science, Burapha University, Chonburi 20131, Thailand.
E-mail address: rungnaph@buu.ac.th (R. Saeeng).

https://doi.org/10.1016/j.bmcl.2021.128135
Received 4 March 2021; Received in revised form 5 May 2021; Accepted 19 May 2021
Available online 24 May 2021

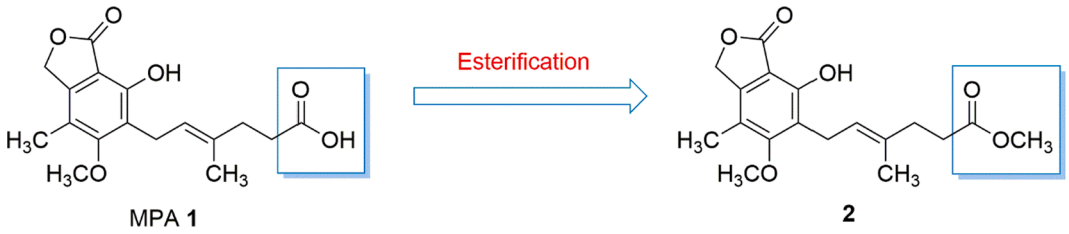

Scheme 1. Esterification of MPA **1.**

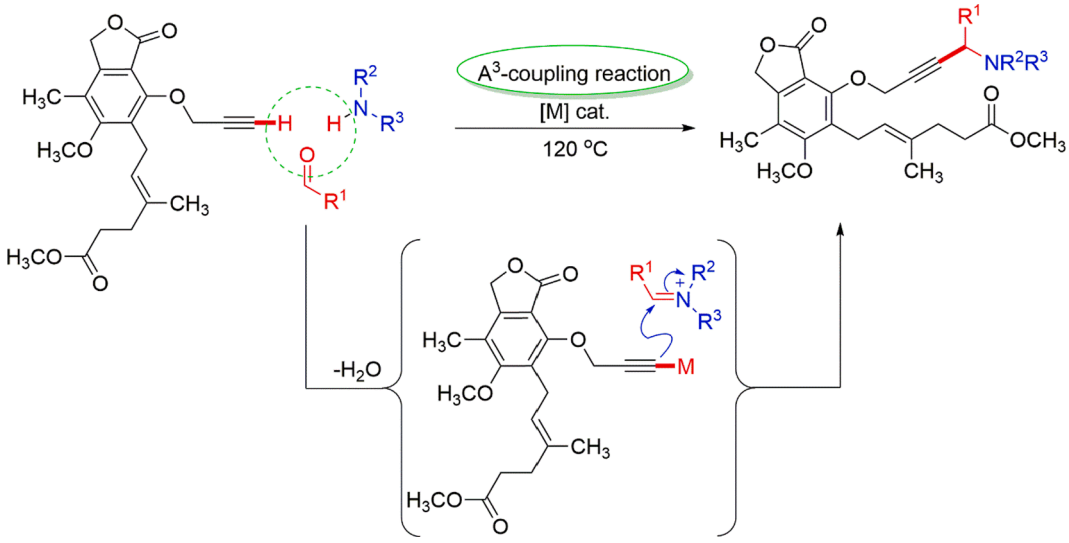

Scheme 2. A^3-coupling reaction for the synthesis of propargylamine mycophenolate.

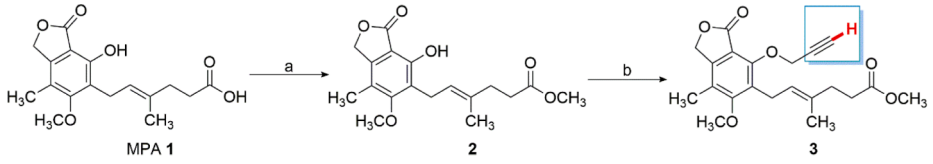

Scheme 3. Synthesis of propargylether mycophenolate **3**[a]. [a]Reaction conditions: a) **1** (0.0062 mol), H_2SO_4 (1.0 mL), CH_3OH (30.0 mL), 6 h, b) propargylbromide (3.0 equiv), K_2CO_3 (3.0 equiv), DCM (30.0 mL), 0 °C-rt, 92%.

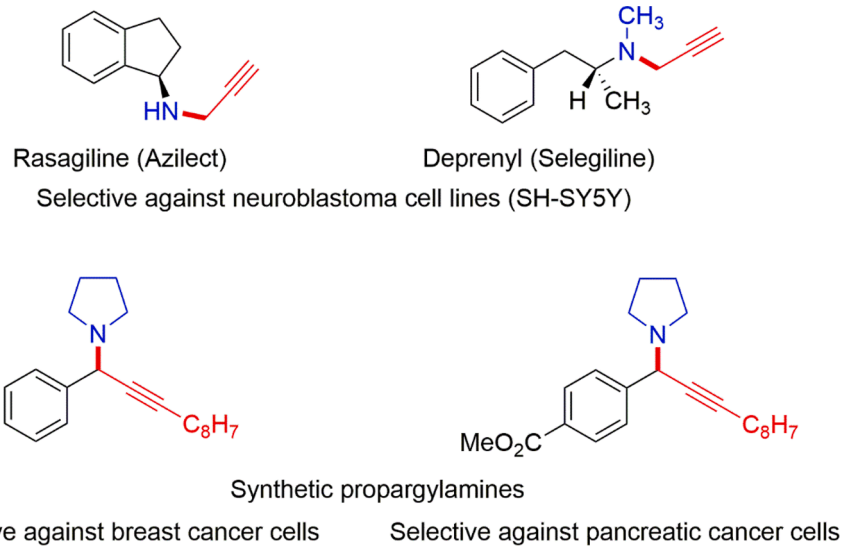

Fig. 1. Some of the representative propargylamine analogues as excellent candidates against different cancer types.

Table 1

Optimization of the synthesis of MPA analog **6a**[a]

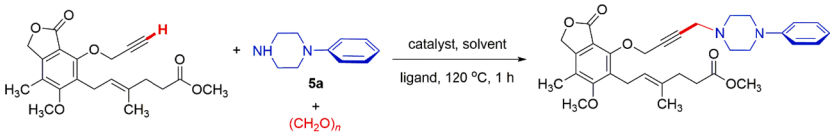

Entry	Catalyst	Ligand	Solvent	Yield [%][b]
1	CuI	–	Toluene	68
2	CuI	–	Dioxane	92
3	CuI	–	THF	24
4	CuI	–	EtOH	20
5	CuI	–	CH_3CN	29
6	CuI	–	DMF	52
7	CuI	–	DMSO	29
8	CuCl	–	Dioxane	70
9	$CuCl_2$	–	Dioxane	80
10	$CuBr_2$	–	Dioxane	70
11	$Cu(OAc)_2$	–	Dioxane	64
12	$CuSO_4$	–	Dioxane	61
13	CuI	2,2′-bipy	Dioxane	45
14	CuI	PPh_3	Dioxane	52
15	$AgNO_3$	–	Dioxane	41
16	AgOAc	–	dioxane	31
17	$ZnCl_2$	–	dioxane	76
18	Zn powder	–	dioxane	NR
19	$NiCl_2$DME	–	dioxane	NR

[a] Reaction conditions: **3** (0.1344 mmol), **4** (0.6720 mmol), **5a** (0.1478 mmol), catalyst (50 mol%), ligand (20 mol%), in solvent (1.0 mL) at the 120 °C for 1 h.

[b] Isolated yields. NR = No reaction.

and noteworthy anticancer activity against neuroblastoma cell lines (SH-SY5Y).[29,30] Two synthetic propargylamines displayed a high degree of cytotoxic selectivity (breast and pancreatic cancer cells). The levels of selectivity give a very interesting perspective for further development of a new anticancer agent.[31]

In this work, we designed and synthesized a series of propargylamine mycophenolate derivatives by A^3-coupling reaction.[32,33] The A^3-coupling methods involves the metal-catalyzed alkyne addition to imines or *in situ* formation of imines derived from amines and aldehydes (Scheme 2). The present study evaluated all synthetic analogues for cytotoxic activity against six cancer cells including neuroblastoma cell (SH-SY5Y).

Preparation of propargylether mycophenolate **3** as the precursor for synthesis of a series of propargylamine mycophenolate is outlined in Scheme 3. Esterification of the MPA **1** with CH_3OH in the presence of H_2SO_4 afforded the methyl mycophenolate **2** followed by propargylation reaction of **2** with propargyl bromide and K_2CO_3 gave compound **3** in 92% yields in two steps.

The A^3-coupling reaction was investigated for synthesis a series of propargylamine mycophenolate **6** by screening several catalysts and solvents to find the optimal condition. Propargylether mycophenolate **3**, formaldehyde **4** and phenylpiperazine **5a** were employed as the model substrates. The reaction was carried out at 120 °C for 1 h and detailed optimization conditions are presented in Table 1.

The A^3-coupling reaction in the presence of catalytic amounts of CuI (50 mol%) in toluene afforded the desired product **6a** in 68% yields (Table 1, entry 1). Interestingly, by changing the solvent to dioxane, we were able to improve product yield significantly to 92% yields (entry 2). Encouraged by this result, reaction was investigated with other solvents including THF, EtOH, CH_3CN, DMF and DMSO (entries 3–7), however, yields were not improved over those with dioxane. Yields with other copper salts, CuCl, $CuCl_2$, $CuBr_2$, $Cu(OAc)_2$, and $CuSO_4$ (entries 8–12), were 70, 80, 70, 64, and 61%. Ligands such as 2,2′-bipy, and PPh_3 did not improve yields of **6a** (entries 13–14). Ag catalysts such as $AgNO_3$ and AgOAc produced lower yields than CuI (entries 15–16). When $ZnCl_2$ was replaced, coupling product **6a** was produced with 76% yield (Table 1, entry 17). No desired product was obtained when Zn powder or $NiCl_2$-DME was used as a catalyst (entries 18–19). The reaction with CuI in dioxane provided optimum conditions for the A^3-coupling reaction with a product yield of 92% (Table 1, entry 2).

Then we explored the scope of reaction using various amine derivatives for synthesizing a series of propargylamine MPA analogues for study the structure activity relationship. This A^3-coupling reaction provides good functional group compatibility and high yields of designed product and water is the only byproduct. Various substituted piperazine were introduced to compound **3** to give the first analogues **6a-6h** in good to excellent yields. The hydroxy- and cyano-phenyl piperazine gave lower yield of **6e** and **6f** comparing to other piperazine. Chloro-benzyl and piperonyl piperazine gave the desired coupling product **6g** and **6h** in high yields. Diphenylpiperazine derivatives served as suitable amine substrates in providing *N*-propargylated products **6i**, **6j**, and **6k** in excellent yields. Acetyl, hydroxyethyl, pyrimidyl, and carbonylbenzodioxane-piperazine gave coupling products **6l**, **6m**, **6n**, and **6p** in up to 80% yields. When this reaction condition was applied to the piperazine bearing pyridine group, the desired product **6o** was not produced probably due to complexation of pyridine with copper (Cu) led to a reduction of reactivity in CuI. The scope of reaction was expanded to piperidine derivatives with various substituents including benzyl group, carboxylic acid, methyl ester and tetrahydroquinoline led to products **6q-6u** in moderate to high yields. All products were well tolerated under the optimized conditions. Morpholine and pyrrolidine were also employed as substrates, affording products **6v** and **6w** in moderate yields. Secondary aliphatic amines provided excellent yields of products **6x-6y**. Also, we found the primary amine gave bis-mycophenolate product **6aa** in moderated yields (Scheme 4).

Cytotoxic activities of mycophenolic acid (MPA **1**) and synthetic analogues were evaluated *in vitro* against selected cancer cell lines including KKU-M213 (human intrahepatic cholangiocarcinoma), FaDu (human squamous cell carcinoma), HT-29 (human colorectal adenocarcinoma), MDA-MB-231 (human mammary gland/breast adenocarcinoma), A-549 (human lung carcinoma), SH-SY5Y (human neuroblastoma), and MMNK-1 (Highly differentiated immortalized human cholangiocyte cell line) in Table 2. MMNK-1 is a healthy cell line reference. Sulforhodamine B (SRB) assay was used to evaluate

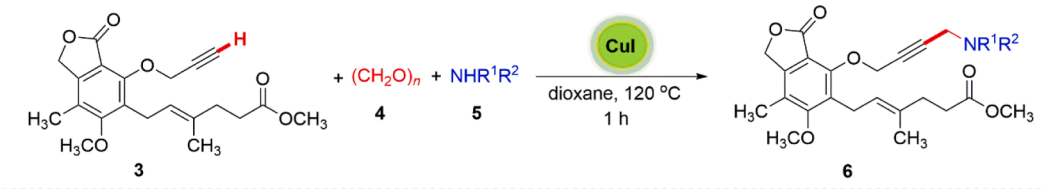

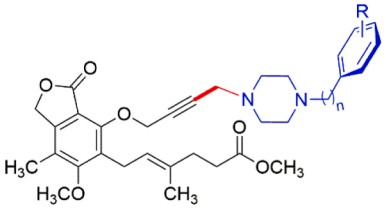

6a: n = 0, R = H (93% yield)
6b: n = 0, R = 2-OCH_3 (99% yield)
6c: n = 0, R = 2-F (99% yield)
6d: n = 0, R = 4-CH_3 (95% yield)
6e: n = 0, R = 4-OH (79% yield)
6f: n = 0, R = 4-CN (78% yield)
6g: n = 1, R = 4-Cl (95% yield)
6h: n = 1, R = 3,4-(OCH_2O) (89% yield)

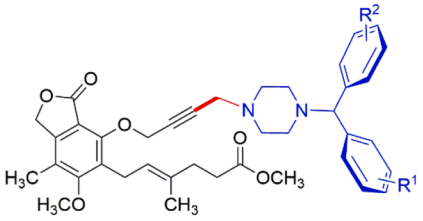

6i: R^1 = H, R^2 = H (95% yield)
6j: R^1 = 4-Cl, R^2 = H (99% yield)
6k: R^1 = 4-F, R^2 = 4-F (99% yield)

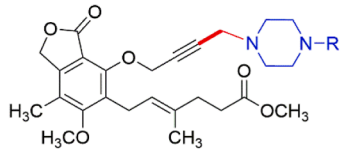

6l: R = Ac (94% yield)
6m: R = CH_2CH_2OH (82% yield)
6n: R = 2-pyrimidine (88% yield)
6o: R = 4-pyridine (NR)
6p: R = carbonylbenzodioxane (81% yield)

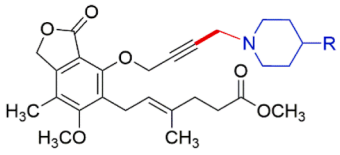

6q: R = Bn (67% yield)
6r: R = CO_2H (78% yield)
6s: R = CO_2CH_3 (82% yield)

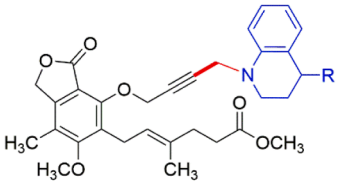

6t: R = H (72% yield)
6u: R = Ph (72% yield)

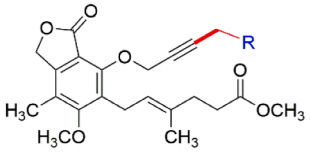

6v: R = morpholine (69% yield)
6w: R = pyrolidine (74% yield)
6x: R = $(CH_3CH_2CH_2CH_2)_2N$ (99% yield)
6y: R = $(CH_2{=}CHCH_2)_2N$ (99% yield)
6z: R = $C_6H_5N(CH_2)_3CH_3$ (66% yield)

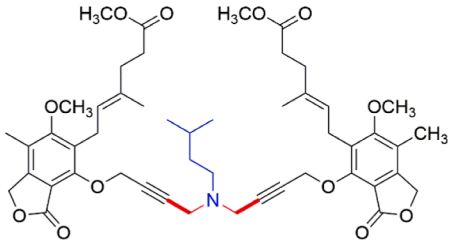

6aa: (50% yield)

Scheme 4. Substrate scope of propargylamine mycophenolate derivatives[a]. [a]Reactions performed on 0.2685 mmol scale of **3**. All isolated yields were based on **3**.

Table 2
In vitro cytotoxicity, of MPA **1**, propargylether-mycophenolate **3** and a series of newly synthesized analogues **6a-6aa.**

Comp.	IC_{50} (μM)[a]						
	KKU-M213	FaDu	HT-29	MDA-MB-231	A-549	SH-SY5Y	MNN-K1
MPA **1**	7.16	6.72	6.48	7.83	1.21	0.56	7.19
2	7.45	6.15	23.73	9.62	0.82	0.26	5.82
3	35.73	15.25	28.79	49.23	31.79	3.07	25.25
6a	>50	>50	>50	>50	21.97	9.14	>50
6b	>50	>50	>50	>50	>50	43.62	>50
6c	>50	>50	>50	>50	45.30	35.78	>50
6d	>50	>50	>50	>50	>50	37.70	>50
6e	>50	>50	>50	>50	>50	46.10	>50
6f	>50	>50	>50	>50	>50	37.79	>50
6g	>50	>50	>50	>50	>50	31.24	>50
6h	>50	>50	>50	>50	45.48	34.80	>50
6i	>50	>50	>50	>50	32.68	23.74	>50
6j	>50	>50	>50	>50	29.06	9.90	>50
6k	>50	>50	>50	>50	34.08	25.83	>50
6l	>50	>50	>50	>50	>50	>50	>50
6m	>50	>50	>50	>50	>50	35.67	>50
6n	>50	>50	>50	>50	>50	>50	>50
6p	>50	>50	>50	>50	>50	>50	>50
6q	>50	>50	>50	>50	40.69	24.50	>50
6r	>50	>50	>50	>50	>50	47.22	>50
6s	>50	>50	>50	>50	40.51	41.16	>50
6t	>50	>50	>50	>50	18.02	9.57	>50
6u	25.92	24.55	39.54	28.66	7.68	6.45	23.29
6v	>50	>50	>50	>50	>50	>50	>50
6w	>50	>50	46.47	>50	35.93	31.08	>50
6x	38.18	30.89	>50	39.78	30.56	21.53	35.99
6y	>50	>50	>50	>50	43.47	36.43	36.43
6z	22.91	21.21	36.71	19.76	6.97	5.96	18.33
6aa	48.32	46.68	>50	48.63	27.52	20.56	48.19
Ellipticine	1.97	1.85	1.95	2.03	1.16	2.13	1.89

[a] IC_{50} values (drug concentration causing 50% growth inhibition) in μM.

cytotoxicity of synthesized compounds. Analogues were dissolved in DMSO (<0.05%). Cytotoxic potency was expressed as the concentration that inhibited 50% of cell viability (IC_{50}, Table 2). Ellipticine was used as a standard drug for comparison.

The cytotoxicity results (IC_{50} values) of MPA **1** and synthetic propargylamine mycophenolate **6a-6aa** were summarized in Table 2. MPA **1** exhibited greater cytotoxic activity than ellipticine on SH-SY5Y cancer cell lines with IC_{50} 0.56 μM and comparable activity on A-549 cell line. Modification by esterification and propargylation of MPA **1** to give propargylether mycophenolate **3** led to a reduction in toxicity to normal cells. Compound **3** showed lower toxicity to normal cells (IC_{50} MNN-K1 = 25.25 μM) but good inhibition against SH-SY5Y (human neuroblastoma) cell line with IC_{50} values 3.07 μM. From this result, the introduction of propargyl moiety may play an important role for selective cytotoxic activity on neuroblastoma. Further modification of this propargyl-MPA scaffold by introducing of various amines led to analogues **6**. Cytotoxic activity of some analogues **6** indicated them to be more selective towards SH-SY5Y cell line and not toxic to normal cells. The first modified phenyl piperazine-propargyl MPA analog **6a** showed selective cytotoxic activity on SH-SY5Y cell line with IC_{50} values 9.14 μM and no toxicity to the normal cells. Substituted phenyl- and benzyl-piperazine-MPA analogues **6b-6f** and **6g-6h** showed lower activity on SH-SY5Y cell than **6a**. However, introducing of diphenyl piperazine on MPA led to compounds **6i-6 k** which showed activity effective than the mono-phenyl piperazine MPA series on SH-SY5Y and A-549 cancer cells. Chlorine analog **6j** demonstrated good selective toxicity on SH-SY5Y cell line with IC_{50} value of 9.90 μM. Piperazine-propargyl MPA scaffolds containing acetyl **6l**, hydroxyethyl **6m**, pyrimidyl **6n**, and carbonylbenzodioxane **6p** did not show any significant activity at concentrations lower than 50 μM. These results indicated the phenyl- and benzyl-substituent on piperazine plays an important role in improving cytotoxicity of MPA. Analogues without these fragment displayed a decrease in activity. The replacement of piperazine on propargyl-MPA scaffold with piperidine bearing benzyl, carboxylic acid and ester **6q-6s** showed the cytotoxicity results to confirm the importance of the benzyl ring on MPA. Benzyl substitution piperidine **6q** displayed greater activity than at other piperidine analogues **6r** and **6s**. Hydroquinoline-MPA **6u** showed significant activity against SH-SY5Y and A549 cell lines with IC_{50} values of 6.45–7.68 and exhibited cytotoxicity against all six cancer cell lines with IC_{50} value below 40.0 μM. Analog **6t** also demonstrated comparable activity against SH-SY5Y and A549 cell lines to that of **6u**. Further modification to study the SAR of propargyl-MPA series by introducing heterocyclic and aliphatic amine led to a series of novel propargyl-MPA bearing morpholine **6v**, pyrrolidine **6w**, aliphatic amine moieties **6x-6z** and bis-MPA analog **6aa**. Butylaniline derivative **6z** showed excellent cytotoxicity with IC_{50} values of 6.97 and 5.96 μM against A-549 cells and the SH-SY5Y cell line and lower toxicity to normal cells than ellipticine.

MPA **1** and mycophenolate **2** exhibited cytotoxic activity against all cancer cell lines especially on A-549 and SH-SY5Y, however both compounds were toxic also to normal cells. Introducing propargyl group led to compound **3** which was selectively toxic to neuroblastoma (SH-SY5Y) cancers cells with an IC_{50} of 3.07 μM but non-toxic to normal cell. A^3-coupling reaction of **3** with various amines led to a series of analogues **6** in which compounds **6a**, **6j**, **6t**, **6u**, and **6z** showed high cytotoxic activity on neuroblastoma (SH-SY5Y) cancers cells but no toxicity to normal cell line (MMNK-1; Fig. 2).

The modification of the piperazine ring by inclusion of a phenyl group and chloro-diphenyl at *N*-4 (compounds **6a** and **6j**) significantly improved cytotoxicity against neuroblastoma (SH-SY5Y) cancer cell lines and was not toxic to the normal cell line (MMNK-1) relative to MPA **1**, compounds **2** and **3** (Fig. 2 and Table 2). Replacement of the piperazine scaffold with hydroquinoline produced analogues **6t** and **6u** that exhibited comparable cytotoxicity to that of **6a** and **6j** on the neuroblastoma cancer cell line. Substituted phenyl-hydroquinoline in compound **6u** and butylaniline **6z** significantly improved their anticancer activity against A-549, while other derivatives reduced their anticancer activity on this cancer cell line. Synthesized compounds **6a**, **6j**, **6t**, **6u**, and **6z** effectively kill lung and neuroblastoma cancer cells at a concentration that is not toxic to normal cells.

Propargylamine MPA analogues was explored for the first time on cytotoxicity to neuroblastoma (SH-SY5Y) cancer cells and confirms the important role played by the molecular docking method in understanding the interaction mode of MPA derivative **6a** as the most selective inhibitor with the three proteins CDK9, EGFR and VEGFR-2. These three proteins have been reported as targets in cancer therapy including neuroblastoma SH-SY5Ycells.[34–36] Cyclin dependent kinases (CDKs) are the serine/threonine kinases group[37] which involved in cell cycle progression and cell proliferation.[38] CDK9 are regulators for the RNA transcription of short-lived Mcl-1 proteins in neuroblastoma SH-SY5Y-cells.[39] The inhibition of CDK9 associated with blocking RNA synthesis can lead to inhibiting neuroblastoma cancer cell growth. Next protein, epidermal growth factor receptor (EGFR) is shown in neuronal origin and various tissues of epithelial and plays a significant role in initiating the signaling that directs growth, proliferation, survival, and differentiation in mammalian cells.[40] The widespread expression of EGFR protein was found in neuroblastoma tissues and cell lines, which is of interested for future treatment of neuroblastoma by targeting this protein.[41,42] The protein, vascular endothelial growth factor receptors (VEGFRs) are tyrosine kinase receptors that play an essential role in controlling the cellular proliferation of the cancer cells including neuroblastoma cells.[43,44] The VEGFRs family consists of three members including VEGFR-2 which plays an important role in cancer angiogenesis. Blocking of EGFR and VEGFR-2 signaling pathway might regulate the growth of neuroblastoma cancer cells which are interesting approaches for cancer therapy.[45,46]

The docking simulations were performed using Autodock 4.2 software as an automated tool for predicting the binding mode by the

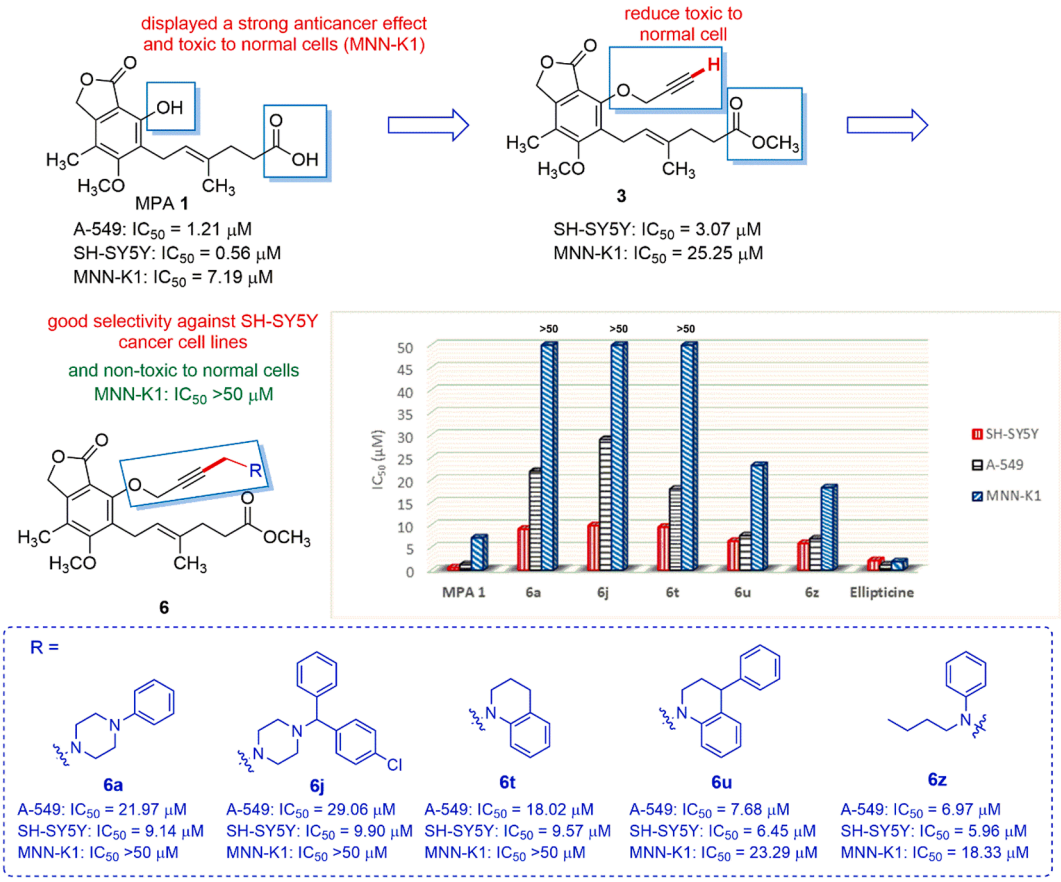

Fig. 2. The propargylamine mycophenolate derivatives showed noteworthy and selective cytotoxicity against lung (A-549) and neuroblastoma (SH-SY5Y) cancers cells.

Table 3
Molecular docking analysis of CDK9/cyclin T with propargylamine-MPA **6a**. The binding energies were evaluated using AutoDock.

Compound	Binding energy (kcal/mol)	Intermolecular hydrogen bonding		Intermolecular hydrophobic contacts
		Amino acids interaction	Distance (Å)	
6a	−13.46	Cys106 Lys151 Asn154	2.89 3.04 2.88	Ile25, Phe105, Ala46, Leu156

Table 4
Molecular docking analysis of EGFR with propargylamine-MPA **6a**. The binding energies were evaluated using AutoDock.

Compound	Binding energy (kcal/mol)	Intermolecular hydrogen bonding		Intermolecular hydrophobic contacts
		Amino acids interaction	Distance (Å)	
6a	−14.06	Met793 Lys721	3.25 3.15	Leu753, Met742, Leu834, Leu764, and Val702

selective analog **6a** (Table 3–5) with the X-ray crystallographic structure of CDK9, EGFR protein kinases and VEGFR-2 receptor, obtained from the Protein Data Bank with PDB code 3LQ5, 4HJO and 4ASD, respectively.

Table 5
Molecular docking analysis of VEGFR-2 with propargylamine-MPA **6a**. The binding energies were evaluated using AutoDock.

Compound	Binding energy (kcal/mol)	Intermolecular hydrogen bonding		Intermolecular hydrophobic contacts
		Amino acids interaction	Distance (Å)	
6a	−16.09	Asp1046 Lys868	3.19 3.36	Cys919, Leu1035, Ala866, Leu889, Val899

Propargylamine-MPA **6a** exhibited the low binding energy values of −13.46 kcal/mol with CDK9 and showed the formation of key hydrogen bonds of the lactone group of MPA interacted with Cys106 residues (Fig. 3). Moreover, the methyl ester group showed hydrogen bonding interaction with Lys151 and Asn154. Interestingly, the phenyl and alkyne moiety in compound **6a** rests in a hydrophobic pocket formed by Ile25, Ala46, and Leu156 as a key residue. Based on the binding interaction, compound **6a** interact with the key amino acid residues at the active site of CDK9.

In order to rationalize the observed SARs, analog **6a** was investigated for the binding orientation with EGRF. Compound **6a** displayed binding energy value of −14.06 Kcal/mol with EGRF (Table 4). The oxygen atom of propargylether and the carbonyl group of ester formed the two hydrogen bonds Met769 and Lys721 residues respectively (Fig. 4). As expectation, the phenyl piperazine of **6a** is located in the active region and promotes hydrophobic interactions with Leu753, Met742, Leu834 and Leu764. Additionally, the propargyl group displayed interactions with Val702.

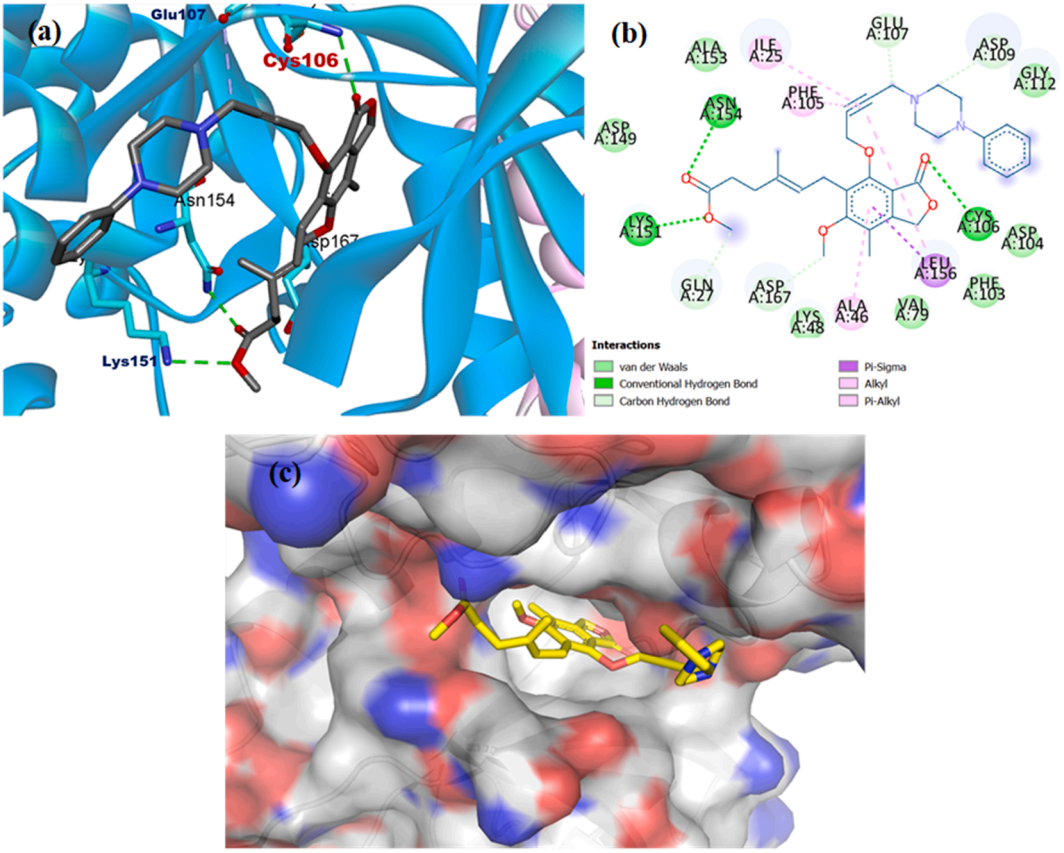

Fig. 3. Docking of **6a** into the active site of CDK9. (a) The protein structure is shown in ribbon and propargylamine-MPA **6a** is shown as stick model. (b) 2D interaction molecular docking diagrams. Hydrogen bonds are shown as green dashed lines. (c) Protein residues are in surface representation.

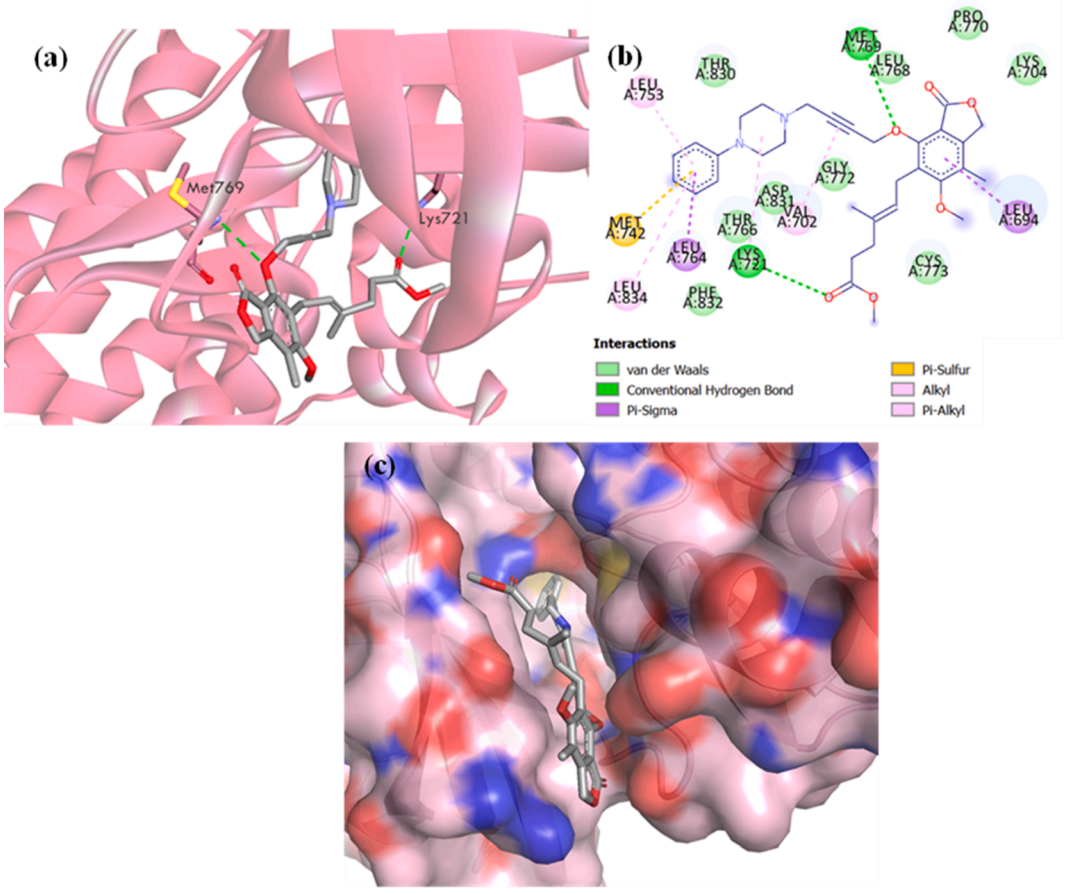

Fig. 4. Docking of **6a** into the active site of EGFR. (a) The protein structure is shown in ribbon and propargylamine-MPA **6a** is shown as stick model. (b) 2D interaction molecular docking diagrams. Hydrogen bonds are shown as green dashed lines. (c) Protein residues are in surface representation.

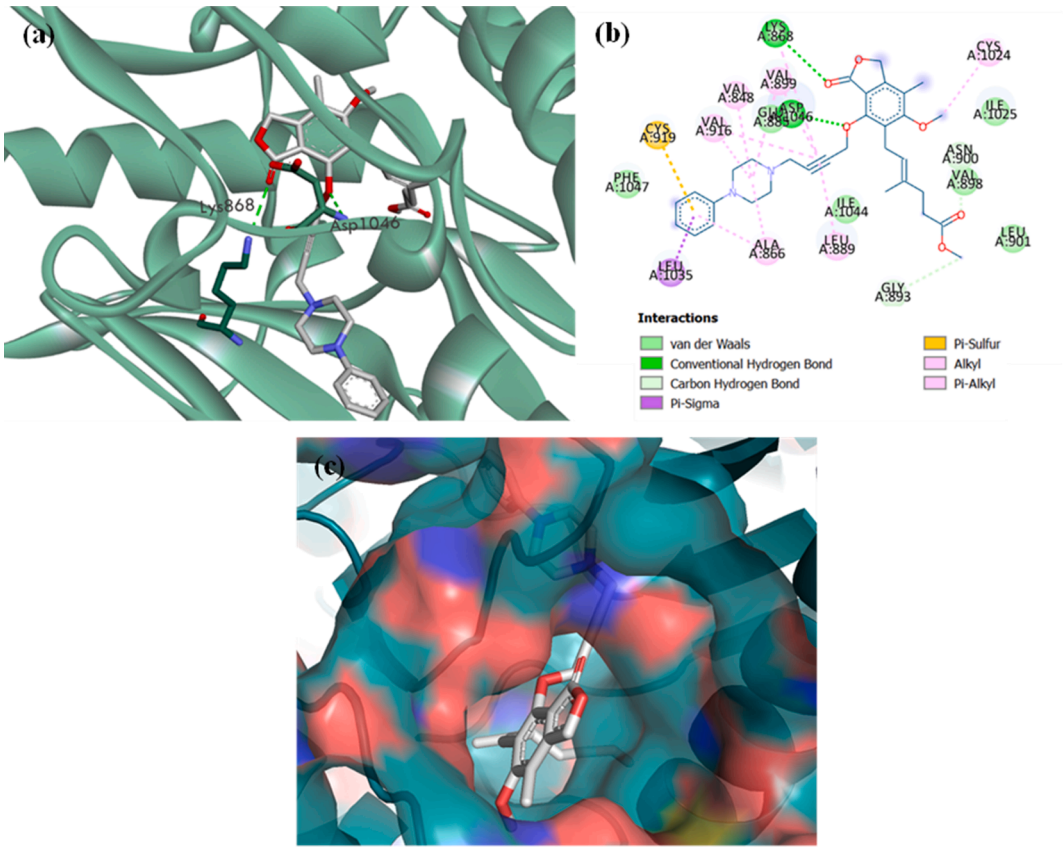

Fig. 5. Docking of **6a** into the active site of VEGFR-2. (a) The protein structure is shown in ribbon and propargylamine-MPA **6a** is shown as stick model. (b) 2D interaction molecular docking diagrams. Hydrogen bonds are shown as green dashed lines. (c) Protein residues are in surface representation.

Similarly, propargylamine-MPA **6a** was investigated for the binding orientation into the active site of VEGFR-2 and exhibited the lowest binding energy −16.09 kcal/mol (Table 5). Compound **6a** displayed the formation of the two hydrogen bonds of the lactone ring with Lys868 and the propargylether with the key amino acid Asp1046 (Fig.5). Other parts of the molecule showed hydrophobic interactions with Cys919 as a key residue, Leu1035, Ala866, Leu889, Val899. These results indicated that propargylamine-MPA **6a** had potential to be the novel VEGFR-2 inhibitors.

Molecular docking simulation with all three proteins supported the observed high activity of **6a**. The propargyl ether and substituted phenyl group of MPA analog **6a** showed a strong hydrogen bond and displayed good hydrophobic interaction while compound **6v** with low cytotoxicity showed less interaction. The calculated binding potential of **6v** comparing with **6a** are represented in Table S1 and Figs. S1-S3. (SI, page S41-S43), which led to a more clear understanding of the cytotoxicity against neuroblastoma SH-SY5Y cell lines provided by these interactions.

In summary, a simple and highly efficient method for the synthesis of propargylamine-MPA analogues through A^3-coupling reaction is reported. It provides good functional group compatibility, atom economy and highly quantitative yields of designed product without a co-catalyst or activator. Water is the only byproduct. All propargylamine MPA analogues were evaluated for their *in vitro* cytotoxity. Among tested compounds, phenylpiperazine MPA **6a**, chloro-diphenylpiperazine MPA **6j**, hydroquinoline MPA **6t** and **6u**, and butylaniline MPA **6z** showed selective and promising inhibition against SH-SY5Y cancer cell lines. They exhibited little evidence of toxicity toward human normal cells relative to MPA **1** and the drug, ellipticine. Computational studies revealed that **6a** possesses a high affinity with CDK9 (−13.46 kcal/mol), EGFR (-14.06 kcal/mol), and VEGFR-2 (−16.09 kcal/mol). Our results demonstrated the propargyl ether and substituted phenyl group of MPA play very significant roles in cytotoxic activity against neuroblastoma SH-SY5Y cell lines. Propargylamine-MPA analogues could serve as a promising candidate for further studies as an anticancer agent against neuroblastoma.

Declaration of Competing Interest

The authors declare that they have no known competing financial interests or personal relationships that could have appeared to influence the work reported in this paper.

Acknowledgements

This project is funded by National Research Council of Thailand (NRCT), The Research Unit in Synthetic Compounds and Synthetic Analogues from Natural Product for Drug Discovery (RSND) and the Center of Excellence for Innovation in Chemistry (PERCH-CIC). R.S. and P.S. are grateful for support through a PhD scholarship from Science Achievement Scholarship of Thailand. The authors would like to thank Assistant Prof. Suchaya Pongsai, Faculty of Science, Burapha University, for a helpful discussion on docking simulations techniques. Special thanks to Prof. Dr Frederick W. H. Beamish, Faculty of Science, Burapha University, for his comments and English correction.

Appendix A. Supplementary data

Supplementary data to this article can be found online at https://doi.org/10.1016/j.bmcl.2021.128135.

References

1 WHO factsheet. https://www.who.int/news-room/fact-sheets/detail/cancer, (2018).
2 Xu S, Yao H, Pei L, et al. Design, synthesis, and biological evaluation of NAD(P)H: Quinone oxidoreductase (NQO1)-targeted oridonin prodrugs possessing indolequinone moiety for hypoxia-selective activation. *Eur J Med Chem.* 2017;132: 310–321. https://doi.org/10.1016/j.ejmech.2017.03.055.
3 Samutprasert P, Chiablaem K, Teeraseranee C, et al. Epigallocatechin gallate-zinc oxide co-crystalline nanoparticles as an anticancer drug that is non-toxic to normal cells. *RSC Adv.* 2018;8(14):7369–7376. https://doi.org/10.1039/C7RA10997K.
4 Ishola TA, Chung DH. Neuroblastoma. *Surg Oncol.* 2007;16(3):149–156. https://doi.org/10.1016/j.suronc.2007.09.005.
5 Paulino AC, Ferenci MS, Chiang K-Y, Nowlan AW, Marcus RB. Comparison of conventional to intensity modulated radiation therapy for abdominal neuroblastoma. *Pediatr Blood Cancer.* 2006;46(7):739–744. https://doi.org/10.1002/pbc.
6 Wagner LM, Danks MK. New therapeutic targets for the treatment of high-risk neuroblastoma. *J Cell Biochem.* 2009;107(1):46–57. https://doi.org/10.1002/jcb.v107:110.1002/jcb.22094.
7 Smith V, Foster J. High-Risk Neuroblastoma Treatment Review. *Children (Basel).* 2018;5(9):114. https://doi.org/10.3390/children5090114.
8 Tibullo D, Giallongo C, Puglisi F, et al. Effect of Lipoic Acid on the Biochemical Mechanisms of Resistance to Bortezomib in SH-SY5Y Neuroblastoma Cells. *Mol Neurobiol.* 2018;55(4):3344–3350. https://doi.org/10.1007/s12035-017-0575-6.
9 Bagnyukova TV, Serebriiskii IG, Zhou Y, Hopper-Borge EA, Golemis EA, Astsaturov I. Chemotherapy and signaling: How can targeted therapies supercharge cytotoxic agents. *Cancer Biol Ther.* 2010;10(9):839–853. https://doi.org/10.4161/cbt.10.9.13738.
10 Ardestani F, Fatemi S-A, Yakhchali B, Hosseyni SM, Najafpour G. Evaluation of mycophenolic acid production by Penicillium brevicompactum MUCL 19011 in batch and continuous submerged cultures. *Biochem Eng J.* 2010;50(3):99–103.
11 Regueira TB, Kildegaard KR, Hansen BG, Mortensen UH, Hertweck C, Nielsen J. Molecular basis for mycophenolic acid biosynthesis in Penicillium brevicompactum. *Appl Environ Microbiol.* 2011;77(9):3035–3043. https://doi.org/10.1128/AEM.03015-10.
12 Shaw LM, Figurski M, Milone MC, Trofe J, Bloom RD. Therapeutic drug monitoring of mycophenolic acid. *Clin J Am Soc Nephrol.* 2007;2(5):1062–1072. https://doi.org/10.2215/CJN.03861106.
13 T.-Y. Wu Y. Peng L.L. Pelleymounter et al. Pharmacogenetics of the mycophenolic acid targets inosine monophosphate dehydrogenases IMPDH1 and IMPDH2: gene sequence variation and functional genomics 161 7 2010 1584 1598 10.1111/j.1476-5381.2010.00987.x.
14 Hodge EE. The role of mycophenolate mofetil in clinical renal transplantation. *World J Urol.* 1996;14:249–255.
15 El-Araby ME, Bernacki RJ, Makara GM, Pera PJ, Anderson WK. Synthesis, molecular modeling, and evaluation of nonphenolic indole analogs of mycophenolic acid. *Bioorg Med Chem.* 2004;12(11):2867–2879. https://doi.org/10.1016/j.bmc.2004.03.048.
16 Yang Na, Wang Q-H, Wang W-Q, et al. The design, synthesis and in vitro immunosuppressive evaluation of novel isobenzofuran derivatives. *Bioorg Med Chem Lett.* 2012;22(1):53–56. https://doi.org/10.1016/j.bmcl.2011.11.078.
17 Iwaszkiewicz-Grzes D, Cholewinski G, Kot-Wasik A, Trzonkowski P, Dzierzbicka K. Synthesis and biological activity of mycophenolic acid-amino acid derivatives. *Eur J Med Chem.* 2013;69:863–871. https://doi.org/10.1016/j.ejmech.2013.09.026.
18 Dun B, Sharma A, Teng Y, et al. Mycophenolic acid inhibits migration and invasion of gastric cancer cells via multiple molecular pathways. *PLoS ONE.* 2013;8(11):e81702. https://doi.org/10.1371/journal.pone.0081702.
19 Felczak K, Vince R, Pankiewicz KW. NAD-based inhibitors with anticancer potential. *Bioorg Med Chem Lett.* 2014;24(1):332–336. https://doi.org/10.1016/j.bmcl.2013.11.005.
20 Koonrungsesomboon N, Ngamphaiboon N, Townamchai N, et al. Phase II, multi-center, open-label, single-arm clinical trial evaluating the efficacy and safety of Mycophenolate Mofetil in patients with high-grade locally advanced or metastatic osteosarcoma (ESMMO): rationale and design of the ESMMO trial. *BMC Cancer.* 2020;20(1). https://doi.org/10.1186/s12885-020-06751-2.
21 Quemeneur L, Flacher M, Gerland LM, Ffrench M, Revillard JP, Bonnefoy-Berard N. Mycophenolic acid inhibits IL-2-dependent T cell proliferation, but not IL-2-dependent survival and sensitization to apoptosis. *J Immunol.* 2002;169(5): 2747–2755. http://www.jimmunol.org/content/169/5/2747.
22 Behrend M. Adverse gastrointestinal effects of mycophenolate mofetil:aetiology, incidence and management. *Drug Saf.* 2001;24(9):645–663. https://doi.org/10.2165/00002018-200124090-00002.
23 Lopez-Solis R, DeVera M, Steel J, et al. Gastrointestinal side effects in liver transplant recipients taking enteric-coated mycophenolate sodium vs. mycophenolate mofetil. *Clin Transplant.* 2014;28(7):783–788. https://doi.org/10.1111/ctr.2014.28.issue-710.1111/ctr.12379.
24 Manger B, Hiepe F, Schneider M, et al. Impact of switching from mycophenolate mofetil to enteric-coated mycophenolate sodium on gastrointestinal side effects in patients with autoimmune disease: a Phase III, open-label, single-arm, multicenter study. Clin Exp Gastroenterol. 2015;8: 205-213. https://doi.org/10.2147/CEG.S81922.
25 Budde K, Curtis J, Knoll G, et al. Enteric-coated mycophenolate sodium can be safely administered in maintenance renal transplant patients: results of a 1-year study. Am J Transplant. 2004;4(2): 237-243. https://doi.org/10.1046/j.1600-6143.2003.00321.x.
26 Meier-Kriesche HU, Davies NM, Grinyo J, et al. Mycophenolate sodium does not reduce the incidence of GI adverse events compared with mycophenolate mofetil. Am J Transplant. 2005;5(5): 1164; author reply 1165-1166. https://doi.org/10.1111/j.1600-6143.2005.00778.x.
27 Bolea I, Gella A, Unzeta M. Propargylamine-derived multitarget-directed ligands: fighting Alzheimer's disease with monoamine oxidase inhibitors. *J Neural Transm (Vienna).* 2013;120(6):893–902. https://doi.org/10.1007/s00702-012-0948-y.
28 Wünsch M, Senger J, Schultheisz P, et al. Structure-Activity Relationship of Propargylamine-Based HDAC Inhibitors. *ChemMedChem.* 2017;12(24):2044–2053. https://doi.org/10.1002/cmdc.201700550.
29 Inaba-Hasegawa K, Akao Y, Maruyama W, Naoi M. Rasagiline and selegiline, inhibitors of type B monoamine oxidase, induce type A monoamine oxidase in human SH-SY5Y cells. *J Neural Transm (Vienna).* 2013;120(3):435–444. https://doi.org/10.1007/s00702-012-0899-3.
30 Wu Y, Shamoto-Nagai M, Maruyama W, Osawa T, Naoi M. Rasagiline prevents cyclosporine A-sensitive superoxide flashes induced by PK11195, the initial signal of mitochondrial membrane permeabilization and apoptosis. *J Neural Transm (Vienna).* 2016;123(5):491–494. https://doi.org/10.1007/s00702-016-1531-8.
31 Martinez-Amezaga M, Giordano RA, Prada Gori DN, et al. Synthesis of propargylamines via the A(3) multicomponent reaction and their biological evaluation as potential anticancer agents. *Org Biomol Chem.* 2020;18(13):2475–2486. https://doi.org/10.1039/D0OB00280A.
32 Choi Y-J, Jang H-Y. Copper-Catalyzed A3-Coupling: Synthesis of 3-Amino-1,4-diynes. *Eur J Org Chem.* 2016;2016(18):3047–3050. https://doi.org/10.1002/ejoc.201600343.
33 Saha TK, Das R. Progress in Synthesis of Propargylamine and Its Derivatives by Nanoparticle Catalysis via A3 coupling: A Decade Update. *ChemistrySelect.* 2018;3(1): 147–169. https://doi.org/10.1002/slct.201702454.
34 Li Y, Guo Q, Zhang C, et al. Discovery of a highly potent, selective and novel CDK9 inhibitor as an anticancer drug candidate. *Bioorg Med Chem Lett.* 2017;27(15): 3231–3237. https://doi.org/10.1016/j.bmcl.2017.06.041.
35 Maiti P, Nand M, Joshi T, Ramakrishnan MA, Chandra S. Identification of luteolin -7-glucoside and epicatechin gallate from Vernonia cinerea, as novel EGFR L858R kinase inhibitors against lung cancer: Docking and simulation-based study. *J Biomol Struct Dyn.*. 2020:1–10 https://doi.org/10.1080/07391102.2020.1784791.
36 Roaiah HM, Ghannam IAY, Ali IH, et al. Design, synthesis, and molecular docking of novel indole scaffold-based VEGFR-2 inhibitors as targeted anticancer agents. *Arch Pharm (Weinheim).* 2018;351(2):1700299. https://doi.org/10.1002/ardp.v351.210.1002/ardp.201700299.
37 Roskoski Jr R. Cyclin-dependent protein serine/threonine kinase inhibitors as anticancer drugs. *Pharmacol Res.* 2019;139:471–488. https://doi.org/10.1016/j.phrs.2018.11.035.
38 Ding L, Cao J, Lin W, et al. The Roles of Cyclin-Dependent Kinases in Cell-Cycle Progression and Therapeutic Strategies in Human Breast Cancer. *Int J Mol Sci.* 2020; 21(6):1960. https://doi.org/10.3390/ijms21061960.
39 Bettayeb K, Baunbaek D, Delehouze C, et al. CDK Inhibitors Roscovitine and CR8 Trigger Mcl-1 Down-Regulation and Apoptotic Cell Death in Neuroblastoma Cells. *Genes Cancer.* 2010;1(4):369–380. https://doi.org/10.1177/1947601910369817.
40 Wee P, Wang Z. Epidermal Growth Factor Receptor Cell Proliferation Signaling Pathways. *Cancers (Basel).* 2017;9(5). https://doi.org/10.3390/cancers9050052.
41 Tamura S, Hosoi H, Kuwahara Y, et al. Induction of apoptosis by an inhibitor of EGFR in neuroblastoma cells. *Biochem Biophys Res Commun.* 2007;358(1):226–232. https://doi.org/10.1016/j.bbrc.2007.04.124.
42 Zheng C, Shen R, Li K, et al. Epidermal growth factor receptor is overexpressed in neuroblastoma tissues and cells. *Acta Biochim Biophys Sin (Shanghai).* 2016;48(8): 762–767. https://doi.org/10.1093/abbs/gmw064.
43 Smith Gina A, Fearnley Gareth W, Tomlinson Darren C, Harrison Michael A, Ponnambalam S. The cellular response to vascular endothelial growth factors requires co-ordinated signal transduction, trafficking and proteolysis. *Biosci Rep.* 2015;35(5). https://doi.org/10.1042/BSR20150171.
44 Beierle EA, Dai W, Langham MR, Copeland EM, Chen MK. VEGF receptors are differentially expressed by neuroblastoma cells in culture. *J Pediatr Surg.* 2003;38(3): 514–521. https://doi.org/10.1053/jpsu.2003.50091.
45 Lindsey S, Langhans SA. Epidermal growth factor signaling in transformed cells. *Int Rev Cell Mol Biol.* 2015;314:1–41. https://doi.org/10.1016/bs.ircmb.2014.10.001.
46 Shibuya M. Vascular Endothelial Growth Factor (VEGF) and Its Receptor (VEGFR) Signaling in Angiogenesis: A Crucial Target for Anti- and Pro-Angiogenic Therapies. *Genes Cancer.* 2011;2(12):1097–1105. https://doi.org/10.1177/1947601911423031.